Electronic Supplementary Material (ESI) for Faraday Discussions.
This journal is © The Royal Society of Chemistry 2017

Electronic Supporting Information: Determining the Composition of the Vacuum-Liquid Interface in Ionic-Liquid Mixtures

E. J. Smoll Jr.,[†] *M. A. Tesa-Serrate,*[‡] *S. M. Purcell,*[‡] *L. D'Andrea,*[§]*,* *D. W. Bruce,*[§] *M. L. Costen,*[‡] *J. M. Slattery,*[§] *T. K. Minton,*[†,*] *and K. G. McKendrick*[‡,*]

[†] Department of Chemistry and Biochemistry, Montana State University, Bozeman, Montana 59717, United States.

[‡] Institute of Chemical Sciences, School of Engineering and Physical Sciences, Heriot-Watt University, Edinburgh, EH14 4AS, United Kingdom

[§] Department of Chemistry, University of York, Heslington, York YO10 5DD, United Kingdom.

Contents

1. Ionic liquid synthesis and characterization

1.1. General considerations

All air-sensitive experimental procedures were performed under an inert atmosphere of nitrogen using standard Schlenk line and glovebox techniques. Toluene was purified with the aid of an Innovative Technologies anhydrous solvent engineering system. Acetonitrile and hexane were purified by distillation over calcium hydride and sodium, respectively. 1-methylimidazole and 1-bromooctane were purified by vacuum distillation using calcium hydride and activated molecular sieves, respectively. NMR spectra were acquired on a JEOL ECX-400 (operating frequencies: 399.78 MHz for ^{1}H, and 376.17 MHz for ^{19}F). Spectra were typically recorded at 295 K unless otherwise stated. ^{1}H NMR spectra were referenced using the chemical shifts of residual protio solvent resonance. Chemical shifts are reported in parts per million. Elemental analysis was carried out on an Exeter Analytical CE-440 elemental analyser. All ionic liquids synthesised are highly hygroscopic and should be stored under an inert atmosphere.

1.2. Preparation of 1-methyl-3-octylimidazolium bromide, [C$_8$mim]Br

An excess of freshly distilled 1-bromooctane (178.9 g, 160 mL, 0.93 mol), distilled 1-methylimidazole (71.1 g, 69 mL, 0.87 mol) and dry toluene (150 mL) were heated at 60 °C under nitrogen overnight. Stirring was stopped after 17 hours. Once the biphasic mixture was allowed to cool down and settle, the top toluene layer was removed *via* cannula transfer. Further removal of the solvent was performed under vacuum at 60 °C to give a yellow oil with a honey-looking appearance. The product was further dried at 60 °C for 4 days (215.6 g, 90% yield). ^{1}H NMR (400 MHz, acetone-d_6, 293 K), δ (ppm): 10.32 (*s*, 1H), 8.07 (*t*, $^4J_{HH}$ = 1.8 Hz, 1H), 7.98 (*t*, $^4J_{HH}$ = 1.8 Hz, 1H), 4.47 (*t*, $^3J_{HH}$ = 7.4 Hz, 2H), 4.12 (*s*, 3H), 1.99-1.92 (*m*, 2H), 1.34-1.26 (*m*, 10H), 0.85 (*t*, $^3J_{HH}$ = 7 Hz, 3H). ^{1}H NMR (400 MHz, D_2O, 294 K), δ (ppm): 7.46 (*d*, $^4J_{HH}$ = 2.0 Hz, 1H), 7.42 (*d*, $^4J_{HH}$ = 2.0 Hz, 1H), 4.16 (*t*, $^3J_{HH}$ = 7.0 Hz, 2H), 3.86 (*s*, 3H), 1.87-1.79 (*m*, 2H), 1.27-1.18 (*m*, 10H), 0.81 (*t*, $^3J_{HH}$ = 7 Hz, 3H).

1.3. Preparation of 1-methyl-3-octylimidazolium bis(trifluoromethylsulfonyl)imide, [C$_8$mim][NTf$_2$]

[C$_8$mim]Br (38.17 g, 0.14 mol) was dissolved in deionised water (100 mL) and then treated with a solution of Li[NTf$_2$] (40.46 g, 0.14 mol) in deionised water (150 mL). A biphasic system instantly formed, which was allowed to stir at room temperature for 2 days. After this time, the IL phase was separated and thoroughly washed with deionised water (5 × 100 mL). Efficient removal of halides was tested by addition of a solution of $AgNO_3$ in deionised water to an aliquot of the aqueous phase from the previous wash. The IL layer was then dried *in vacuo* (~10^{-3} mbar) at 60 °C for 24 hours to afford the product as a colourless oil (59.0 g, 90% yield). ^{1}H NMR (400 MHz, acetone-d_6, 294 K), δ (ppm): 9.09 (*s*, 1H), 7.81 (*t*, $^4J_{HH}$ = 1.8 Hz, 1H), 7.75 (*t*, $^4J_{HH}$ = 1.8 Hz, 1H), 4.39 (*t*, $^3J_{HH}$ = 7.4 Hz, 2H), 4.09 (*s*, 3H), 1.96 (*br quint*, $^3J_{HH}$ = 7.4 Hz, 2H), 1.39-1.27 (*m*, 10H), 0.86 (*t*, $^3J_{HH}$ = 7 Hz, 3H).

1.4. Preparation of 1-(1*H*,1*H*,2*H*,2*H*,perfluorooctyl)-3-methylimidazolium bis(trifluoromethylsulfonyl)imide, [C_8mimF_{13}][NTf_2]

To a solution of distilled 1-methylimidazole (14.42 g, 14 mL, 0.18 mol) in dry acetonitrile (400 mL) a slight excess of 1*H*,1*H*,2*H*,2*H*-perfluorooctyl iodide (90.90 g, 47 mL, 0.19 mol) was added. The resulting yellowish solution was heated to reflux under nitrogen. Progression of the reaction was followed by ^{1}H NMR. After 8 days, the red solution obtained was concentrated to dryness and the resulting residue washed with dry hexane (5 × 80 mL) *via* cannula transfer. The yellow solid obtained, which corresponds to impure [C_8mimF_{13}]I (76 g), was dried at 60 °C for 1 h. The solid was then suspended in deionised water (200 mL) and treated with a solution of Li[NTf_2] (39.64 g, 0.14 mol) in deionised water (100 mL). A biphasic system instantly formed, which was stirred at room temperature for 3 days, protected from light. After this time, the ionic liquid was extracted with DCM (100 mL) and subsequently washed with deionised water (4 × 100 mL). After removing the dichloromethane under reduced pressure, the orange oil obtained was redissolved in acetonitrile (20 mL). In order to remove the I_2/[I_3]$^-$ impurities from the sample, an aqueous solution of $Na_2S_2O_3$ (1M, 50 mL) was added to the flask, which produced discoloration of the solution from light orange to yellow. Dichloromethane (20 mL) was then poured into the flask and the biphasic solution was vigorously stirred for 1-2 hours. The organic layer was separated and the solvent removed *in vacuo*. Treatment with $Na_2S_2O_3$ was repeated 3 more times. After removal of the solvent, the viscous oil obtained was redissolved in ethyl acetate (25 mL) and thoroughly washed with deionised water (9 × 100 mL). Efficient removal of halides was tested by addition of a solution of $AgNO_3$ in deionised water to an aliquot of the aqueous phase from the previous wash. An aliquot of the ionic liquid phase was also tested (addition of a few drops of acetonitrile is required for this test). The halide-free IL layer was concentrated to dryness and thoroughly dried *in vacuo* (~10^{-3} mbar) at 60 °C for 6 days to afford the product as a light orange oil (66.0 g, 53% yield). Purity of the title compound was checked by elemental analysis. ^{1}H NMR (400 MHz, acetone-d_6, 295 K), δ (ppm): 9.15 (*s*, 1H), 7.90 (*t*, $^4J_{HH}$ = 1.8 Hz, 1H), 7.73 (*t*, $^4J_{HH}$ = 1.8 Hz, 1H), 4.82 (*t*, $^3J_{HH}$ = 6.8 Hz, 2H), 4.08 (*s*, 3H), 3.16-3.03 (*m*, 2H). ^{19}F NMR (376 MHz, acetone-d_6, 295 K), δ (ppm): –80.0 (*s*, NTf_2^-), –81.8 (*t*, $^3J_{FF}$ = 9.8 Hz, CF_3), –114.5 (*quint*, *J* = 15.8 Hz, CF_2), –122.4 (*br s*, CF_2), –123.5 (*br s*, CF_2), –124.2 (*br s*, CF_2), –(126.8-126.9) (*m*, CF_2). Anal. Calcd for $C_{14}H_{10}F_{19}N_3O_4S_2$: C, 23.71; H, 1.42; N, 5.92. Found: C, 23.67; H, 1.35; N, 5.90.

1.5. Commercial ionic liquid characteristics

The ionic liquids were supplied by IoLiTec (Germany) and used as received; their physical properties as stated by the manufacturer are shown in table S1.

Liquid	Purity	[H_2O]	[Halides]
[C_6mim][NTf_2]	>99%	70 ppm	<100 ppm
[C_6mim][BF_4]	>99%	150 ppm	<100 ppm
[C_8mim][NTf_2]	>99%	53 ppm	<100 ppm

Table S1: Ionic liquid physical properties.

2. Surface tension measurements

2.1. Surface tension results [C_2mim]$_{(1-x)}$[C_{12}mim]$_x$[NTf_2]

x	Surface Tension / mN m^{-1}	1σ SEM	S_2	1σ SEM
0	35.24	0.02	0.000	0.004
0.01	34.91	0.03	0.060	0.006
0.04	34.36	0.03	0.162	0.006
0.08	33.74	0.02	0.274	0.003
0.16	32.79	0.02	0.448	0.003
0.24	32.17	0.04	0.561	0.007
0.32	31.92	0.01	0.606	0.002
0.43	31.50	0.01	0.683	0.002
0.52	30.88	0.05	0.795	0.008
0.63	30.71	0.01	0.827	0.003
0.74	30.53	0.05	0.859	0.010
0.87	30.32	0.04	0.898	0.007
0.92	29.91	0.05	0.972	0.009
0.96	30.08	0.04	0.942	0.007
0.99	30.06	0.15	0.945	0.027
1.00	29.76	0.04	1.000	0.007

Table S2: Surface tension results from $[C_2mim]_{(1-x)}[C_{12}mim]_x[NTf_2]$ for multiple bulk mole fraction, *x*.

2.2. Surface tension results $[C_8mim][NTf_2]$ and $[C_8mimF_{13}][NTf_2]$

Liquid	Surface Tension / mN m^{-1}	1σ SEM
$[C_8mim][NTf_2]$	30.42	0.09
$[C_8mim\text{-}F][NTf_2]$	21.90	0.02

Table S3: Surface tensions of neat ionic liquids $[C_8mim][NTf_2]$ and $[C_8mim\text{-}F][NTf_2]$.

3. RAS-LIF rotational distributions

3.1. $[C_8mim]_{0.5}[C_8mimF_{13}]_{0.5}[NTf_2]$ and $[C_8mim][NTf_2]$ rotational spectra

OH rotational excitation spectra were recorded from $[C_8mim]_{(1-x)}[C_8mimF]_x[NTf_2]$ for $x = 0$ and $x = 0.5$. A step size of 0.0020 nm was used and data were collected for 40 laser shots at each step. The photolysis-probe delay was fixed at 12 µs corresponding to the peak of the appearance profile. This process was repeated five times for $x = 0$ and eight times for $x = 0.5$ to account for the much lower OH signal from this mixture. Spectra were recorded on the Q_1 and R_1 branches up to $N = 5$, where N is the sum of the electron orbital quantum and rotational quantum numbers.

3.2. $[C_6mim][BF_4]_{(1-x)}[NTf_2]_x$ rotational spectra

OH excitation spectra were recorded from the pure liquids only, under the assumption that the populations corresponding to the liquid mixtures would not change. A step size of 0.0025 nm was used and data were collected for 20 or 30 laser shots at each step. The photolysis-probe delay was fixed at 15 µs. Six spectra were recorded from $[C_6mim][NTf_2]$ and five from $[C_6mim][NTf_2]$. Spectra were recorded on the Q_1 and R_1 branches up to $N = 4$.

3.3. Rotational analysis

LIFBASE[1] was used the fit the spectra for all liquids, the resultant populations were normalized over the number of respective rotational levels sampled. Figure S1 shows the normalized Q_1 branch populations up to $N = 5$ from $[C_8mim]_{(1-x)}[C_8mimF]_x[NTf_2]$. Figure S2 shows the normalized Q_1 populations from the pure liquids $[C_6mim][BF_4]$ and $[C_6mim][NTf_2]$, up to $N = 4$. The R_1 branch for each mixture system showed similar results. Error bars on figures S1 and S2 are standard error of the mean (SEM).

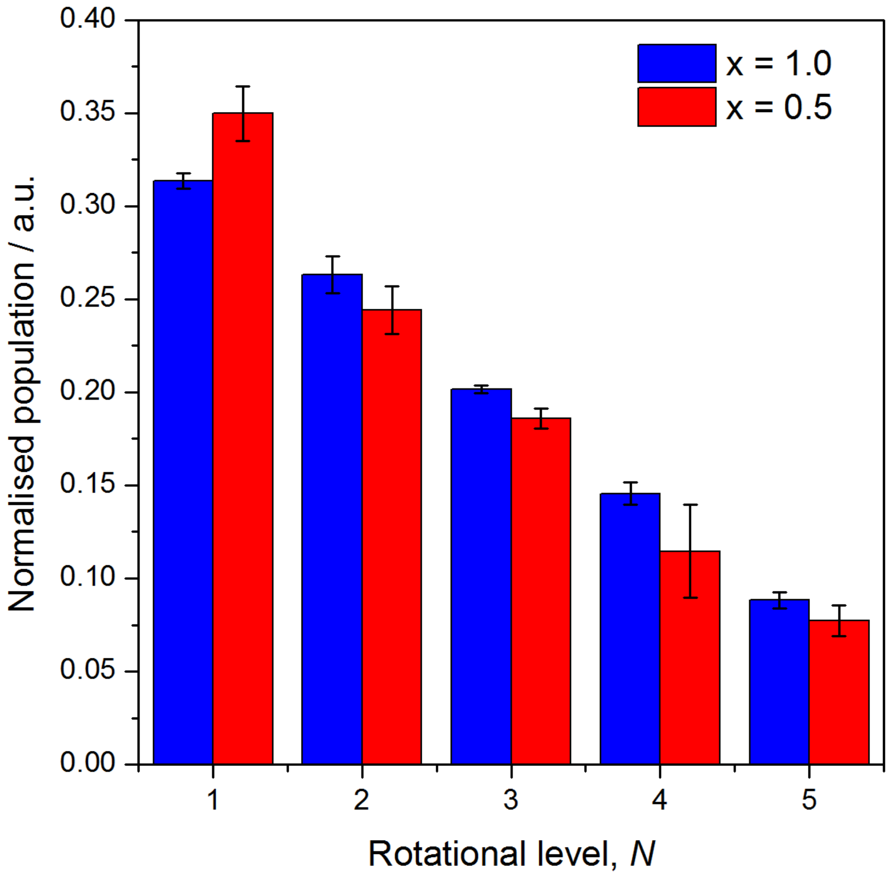

Figure S1: Normalised OH rotational populations from [C_8mim][NTf_2] (x = 1.0) and with bulk mole fraction, x = 0.5, corresponding to [C_8mimF_{13}]$_{0.5}$[C_8mim]$_{0.5}$[NTf_2]. Error bars are 1σ SEM.

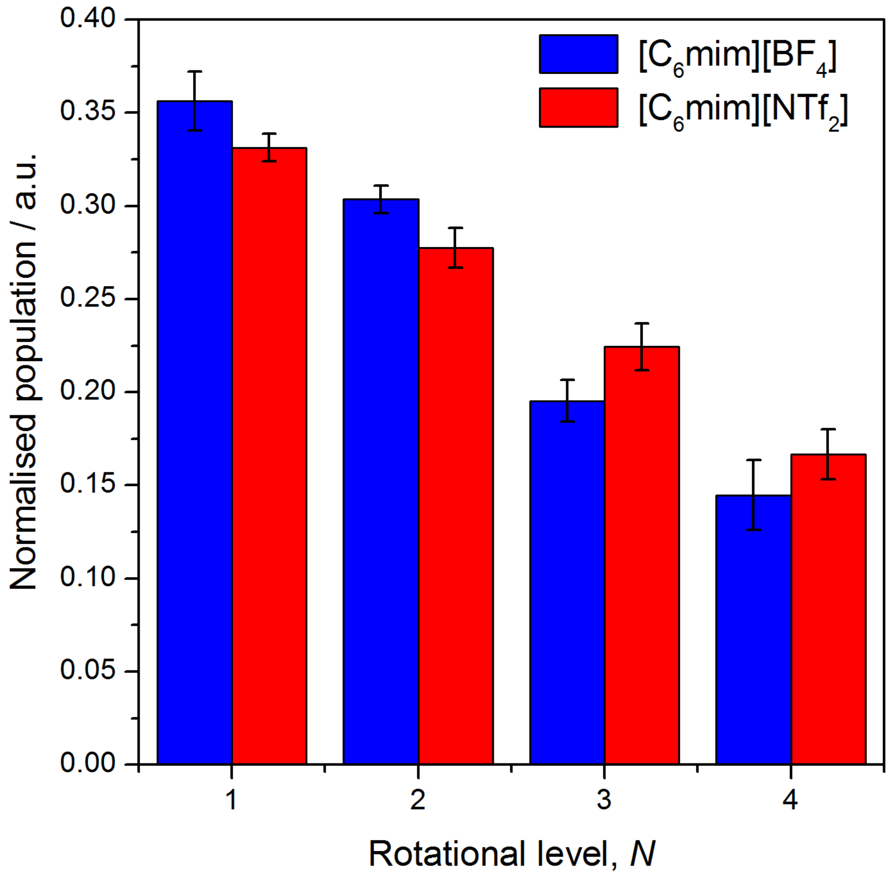

Figure S2: Normalised OH rotational populations from [C_6mim][BF_4] and [C_6mim][NTf_2]. Error bars are 1σ SEM.

4. RAS-LIF appearance profiles for $[C_6mim][BF_4]_{(1-x)}[NTf_2]_x$

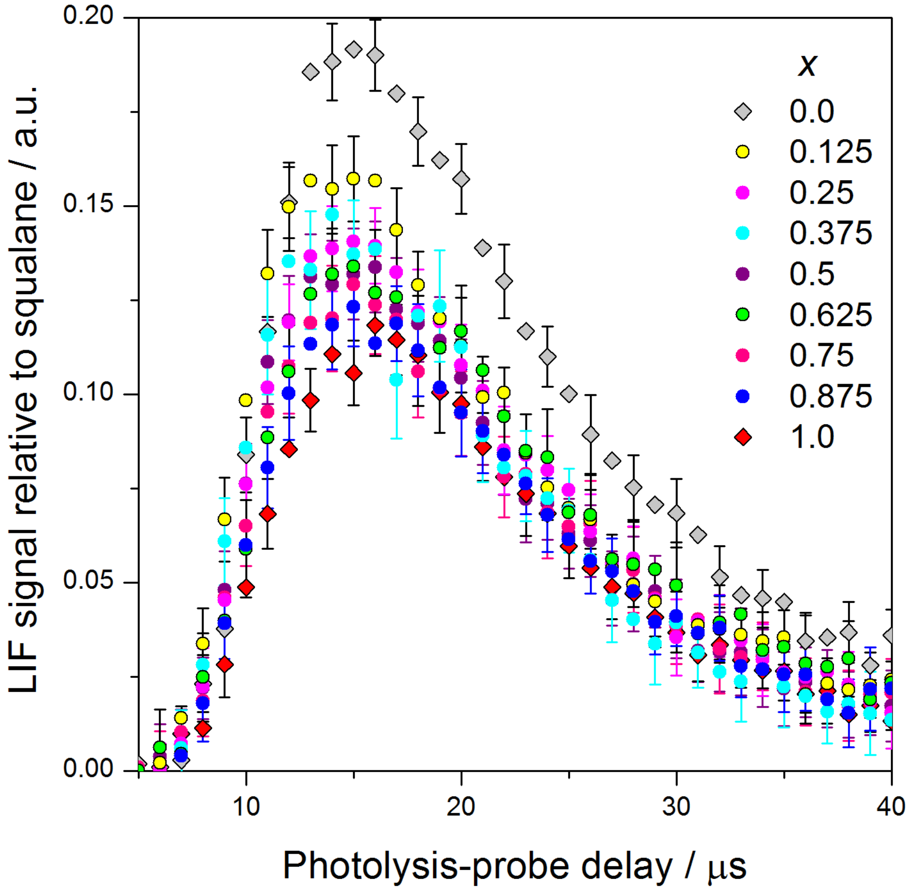

Figure S3: RAS-LIF appearance profiles from $[C_6mim][BF_4]_{(1-x)}[NTf_2]_x$ for multiple bulk mole fractions, x. Error bars are 1σ SEM.

Figure S3 shows the RAS-LIF appearance profiles for the anion mixtures $[C_6mim][BF_4]_{(1-x)}[NTf_2]_x$ recorded on the $Q_1(1)$ line. Some error bars have been omitted for clarity.

5. Integrated RAS-LIF OH density and relative surface exposure values

5.1. Cations mixtures $[C_2mim]_{(1-x)}[C_{12}mim]_x[NTf_2]$

Previously published results[2] show tabulated values for OH flux relative to squalane with bulk mole fraction x, for $[C_2mim]_{(1-x)}[C_{12}mim]_x[NTf_2]$ mixtures. Here, in order to easily compare with the other mixture systems, OH densities, relative to squalane are used. The

OH density for a given x is directly related to OH flux via a constant scale factor as described previously[3]. OH densities for $[C_2mim]_{(1-x)}[C_{12}mim]_x[NTf_2]$ are shown in table S4.

x	OH Density	1σ SEM	S_2	1σ SEM
0.000	0.008	0.005	0.000	0.009
0.010	0.042	0.002	0.062	0.004
0.040	0.099	0.004	0.165	0.008
0.080	0.181	0.003	0.314	0.006
0.160	0.308	0.005	0.545	0.008
0.240	0.400	0.009	0.713	0.016
0.320	0.401	0.006	0.714	0.010
0.430	0.433	0.006	0.773	0.011
0.520	0.429	0.008	0.765	0.015
0.630	0.481	0.006	0.859	0.011
0.740	0.488	0.009	0.872	0.016
0.870	0.507	0.010	0.906	0.019
1.000	0.558	0.009	1.000	0.016

Table S4: Relative OH density and S_2 values for $[C_2mim]_{(1-x)}[C_{12}mim]_x[NTf_2]$ mixtures for multiple bulk mole fractions, x.

5.2. $[C_8mim]_{(1-x)}[C_8mimF_{13}]_x[NTf_2]$

For $[C_8mim]_{(1-x)}[C_8mimF_{13}]_x[NTf_2]$, with bulk mole fraction x, the integrated OH densities were calculated by integrating the OH appearance profiles between 6 μs and 30 μs with a 1 μs step size. The OH densities, S_2 values and associated 1σ SEM are shown in table S5.

To estimate the uncertainty in the experiments, $[C_8mim][NTf_2]$ was measured at the start of the experiments and at the end (after all other liquids had been measured), when a fresh sample of $[C_8mim][NTf_2]$ was loaded. This liquid was also measured alongside a commercial sample of $[C_8mim][NTf_2]$, which was loaded into a separate liquid bath. The physical properties of this sample are shown in table S1. The reported OH density for $[C_8mim][NTf_2]$ in table S5 is a weighted average (instrumental weighting, $1/\sigma^2$) of these three measurements. The three individual measurements are shown in table S6, with the commercial sample giving a slightly higher value of OH density.

x	OH Density	1σ SEM	S_2	1σ SEM
0.000	0.338	0.001	0.000	0.004
0.050	0.226	0.002	0.325	0.007
0.100	0.183	0.002	0.448	0.005
0.250	0.125	0.001	0.618	0.004
0.370	0.086	0.002	0.730	0.005
0.500	0.073	0.006	0.767	0.017
0.750	0.044	0.001	0.851	0.003
0.830	0.041	0.001	0.861	0.004
1.000	-0.007	0.006	1.000	0.018

Table S5: OH density and S_2 values for $[C_8mim]_{(1-x)}[C_8mimF_{13}]_x[NTf_2]$ mixtures for multiple bulk mole fractions, x.

Measurement	OH Density	1σ SEM
1	0.3196	0.0065
2	0.3170	0.0022
Commercial Sample	0.3555	0.0020
Weighted Average	0.3376	0.0014

Table S6: Repeat measurements on $[C_8mim][NTf_2]$ and resulting weighted average.

5.3. $[C_6mim][BF_4]_{(1-x)}[NTf_2]_x$

For the anion mixtures, $[C_6mim][BF_4]_{(1-x)}[NTf_2]_x$, where x is bulk mole fraction, the OH densities were calculated by integrating the appearance profiles in figure S3 between 0 µs and 30 µs with a 1 µs interval. The resulting OH densities and S_2 values are shown in table S7.

x	OH Density	1σ SEM	S_2	1σ SEM
0.000	0.189	0.005	0.000	0.065
0.125	0.160	0.005	0.393	0.067
0.250	0.146	0.005	0.579	0.066
0.375	0.140	0.006	0.665	0.076
0.500	0.134	0.003	0.734	0.042
0.625	0.138	0.006	0.682	0.080
0.750	0.132	0.005	0.770	0.071
0.875	0.122	0.005	0.897	0.069
1.000	0.115	0.004	1.000	0.055

Table S7: OH densities and S_2 values for $[C_6mim][BF_4]_{(1-x)}[NTf_2]_x$ for multiple bulk mole fractions, x.

6. Fitting

6.1. Parameters

All fitting was done in OriginPro 8.6 with equally weighted data points. Parameters from fitting to the RAS-LIF data from the three mixture systems are shown in tables S8-S10. Reported error is standard error of the mean.

Model	Eqn.	Parameter		
Extended Langmuir	5	$\beta = 3.235 \pm 0.297$		
Porter	7	$\beta = 1.147 \pm 0.302$	$A = 1.147 \pm 0.248$	
Margules	9	$\beta = 0.77 \pm 0.112$	$A_1 = 1.315 \pm 0.116$	$A_2 = 1.919 \pm 0.137$

Table S8: Fit parameters from $[C_2mim]_{(1-x)}[C_{12}mim]_x[NTf_2]$ mixtures for different models.

Model	Eqn.	Parameter		
Extended Langmuir	5	β = 5.030 ± 0.836		
Porter	7	β = 1.638 ± 0.205	A = 1.108 ± 0.270	
Margules	9	β = 1.357 ± 0.299	A_1 = 1.687 ± 0.163	A_2 = 1.220 ± 0.283

Table S9: Fit parameters from [C_8mim]$_{(1-x)}$[C_8mimF_{13}]$_x$[NTf_2] mixtures.

Model	Eqn.	Parameter		
Extended Langmuir	5	β = 2.111 ± 0.385		
Porter	7	β = 0.592 ± 0.076	A = 1.681 ± 0.113	
Margules	9	β = 0.504 ± 0.076	A_1 = 1.614 ± 0.112	A_2 = 1.897 ± 0.154

Table S10: Fit parameters from [C_6mim][BF_4]$_{(1-x)}$[NTf_2]$_x$ mixtures.

Fitting parameters for surface tension data acquired from [C_2mim]$_{(1-x)}$[C_{12}mim]$_x$[NTf_2] are shown in table S11.

Model	Eqn.	Parameter		
Piñeiro	11	β = 2.178 ± 0.146	α = 1.000 ± 0.067	
Oliveira	13	A_0 = 1.001 ± 0.065	A_1 = 1.138 ± 0.125	A_2 = 0.591 ± 0.264

Table S11: Fit parameters surface tension measurement from [C_2mim]$_{(1-x)}$[C_{12}mim]$_x$[NTf_2] for Piñeiro and Oliveira models.

6.2. Redlich-Kister molar surface area fit

Equation 16 given in the manuscript is in absolute units with the form,

$$\frac{n_2^s}{A} = \frac{\Gamma_2^{(1)} + \frac{1}{A_1^s}\frac{x_2}{x_1}}{1 + \frac{A_2^s}{A_1^s}\frac{x_2}{x_1}} , \qquad \textbf{(1)}$$

where, n_2^s/A has units of mol m^{-2}. The RAS-LIF signal is proportional to this quantity, therefore equation 1 is re-written as

$$\frac{n_2^s}{A} = \frac{1}{\alpha}\frac{\Gamma_2^{(1)} + \mathrm{C}_1\frac{x_2}{(1-x_2)}}{1 + \mathrm{C}_2\frac{x_2}{(1-x_2)}}, \qquad \textbf{(2)}$$

where α is a dimensionless constant which takes into account experimental parameters, detector efficiency etc., $\mathrm{C}_1 = 1/A_1^s$ and $\mathrm{C}_2 = A_2^s/A_1^s$. In the limit $x_2 \to 1$, equation 2 asymptotically approaches $1/\alpha A_2^s$. This represents the RAS-LIF signal for the more surface active component of the mixture and corresponds to the RAS-LIF signal from [C_{12}mim][NTf_2] in this case. Dividing both sides by this limit, thus normalizing the RAS-LIF signal, α is cancelled and the absolute units of equation 2 are converted into surface exposure, S_2, such that

$$S_2 = \left(\frac{\mathrm{C}_2}{\mathrm{C}_1}\right)\left(\frac{\Gamma_2^{(1)} + \mathrm{C}_1\frac{x_2}{(1-x_1)}}{1+\mathrm{C}_2\frac{x_2}{(1-x_1)}}\right). \qquad \textbf{(3)}$$

This equation is fitted to the RAS-LIF data. Note also, when $x_2 \to 1$, $S_2 \to 1$, constraining the fit.

7. References

1. Luque, J.; Crosley, D. R. *LIFBASE: Database and spectral simulation (version 1.5)*, SRI International Report MP 99-009: 1999.

2. Bruce, D. W.; Cabry, C. P.; Nuno Canongia Lopes, J.; Costen, M. L.; D'Andrea, L.; Grillo, I.; Marshall, B. C.; McKendrick, K. G.; Minton, T. K.; Purcell, S. M.; Rogers, S. E.; Slattery, J. M.; Shimizu, K.; Smoll, E.; Tesa-Serrate, M. A. Nano-Segregation and Structuring in the Bulk and at the Surface of Ionic-Liquid Mixtures. *The Journal of Physical Chemistry B* **2017**. DOI: 10.1021/acs.jpcb.7b01654

3. Tesa-Serrate, M. A.; Marshall, B. C.; Smoll, E. J.; Purcell, S. M.; Costen, M. L.; Slattery, J. M.; Minton, T. K.; McKendrick, K. G. Ionic Liquid–Vacuum Interfaces Probed by Reactive Atom Scattering: Influence of Alkyl Chain Length and Anion Volume. *J. Phys. Chem. C* **2015,** *119* (10), 5491-5505.